JOURNAL OF COMPUTATIONAL PHYSICS 12, 247–268 (1973)

"Energy-Conserving" Plasma Simulation Algorithms*

A. BRUCE LANGDON

Lawrence Livermore Laboratory, University of California, Livermore, California 94550

Received December 4, 1970

Lewis has found algorithms for many-particle plasma simulation models in which there exists an exact energy constant in the limit of small time step. The requirements for energy conservation are examined here and relaxed from those given by Lewis, in that his prescription for the difference form of Poisson's equation is found not necessary. One may therefore choose the Poisson algorithm to satisfy other criteria. However a connection is established between Lewis' difference equation, the interpolation method, and the accuracy of the Coulomb interparticle forces. Unlike the usual models, momentum is not conserved by these algorithms. Rough measures are given for the importance of this nonconservation, in the simplest case of linear interpolation. Another example uses spline interpolation to obtain smoother and more accurate fields and better momentum conservation.

I. INTRODUCTION

Lewis has derived a new class of many-particle plasma simulation models from a Lagrangian formulation [1]. Because the models possess time-independent Hamiltonians, they conserve energy exactly (to the extent that the time integration is accurate). This is to be contrasted to the more usual models for which it can be shown that no combination of the particle kinetic energy with field quantities defined on the spatial grid (charge density, potential, and electric field) is an exact constant [2].

In addition, these models have become of interest because they also apparently suffer less from nonphysical instabilities than do the usual models [2–4]. For these reasons we have studied Lewis' models further.

One interesting aspect of Lewis' derivation was that for each method of interpolation between the particles and the spatial grid there emerged a specific finite-difference form of Poisson's equation. After seeing Lewis' work, the author found a different derivation of the energy-conserving models; this is discussed in [2] as

* Work performed under the auspices of the U.S. Atomic Energy Commission at the Electronics Research Laboratory, University of California, Berkeley [under contract AT-(04-3)-34 (Proj. 128)] and at the Lawrence Livermore Laboratory, Livermore, California.

581/12/2-7

an application of the formalism developed there for other purposes. No restriction to a particular Poisson equation was found necessary to insure energy conservation. However, the Lagrangian has built into it a specific force law which Lewis' formalism takes into account in prescribing the Poisson equation, in a manner to be shown in this paper.

Reference [2] also remarked that the model does not conserve momentum, as exemplified microscopically by the force on a particle due to its own field (the usual models do conserve momentum). Macroscopically, examples are given in which a change in the total particle momentum should be easily noticed. This nonconservation is not unexpected, since the Hamiltonian is not invariant under displacement. Better understanding is desirable here.

This paper reconsiders the requirements for energy conservation in a simpler manner than in [1, 2]. Then a connection is established between Lewis' Poisson operator and the accuracy of the force law. A relation is found between the sampling phenomenon known as "aliasing" and the failure of momentum conservation. Examples of the latter are given; in particular we elaborate on the nature and magnitude of the self-force in the linear interpolation case. Finally, we show how improved algorithms may be derived, giving details in one example.

II. The Algorithm

We first outline the model algorithm and our notation, following Ref. [2] except for the replacement of S_c by S. The charge density defined on the grid points is

$$\rho_{\mathbf{j}} = \sum_i q_i S(\mathbf{X}_{\mathbf{j}} - \mathbf{x}_i). \tag{1}$$

The sum is over particles with charges q_i and positions $\mathbf{x}_i$. The grid points are labelled by the vector $\mathbf{j}$ whose components are integers. The location of grid point $\mathbf{j}$ is $\mathbf{X}_{\mathbf{j}}$. The interpolation function S is usually symmetric and can be regarded as the shape of a finite-size particle. Some modification may be necessary at boundaries.

The electric potential, also defined on the grid, is the solution of a discrete analogue to Poisson's equation, and is a linear combination of the $\{\rho_{\mathbf{j}}\}$ and the boundary conditions if the latter are inhomogeneous. We therefore write the potential as

$$\phi_{\mathbf{j}} = V_c \sum_{\mathbf{l}} g_{\mathbf{j},\mathbf{l}} \rho_{\mathbf{l}} + \phi_{\mathbf{j},\text{ext}}, \tag{2}$$

where $g_{\mathbf{j},\mathbf{l}}$ is the Green's function for the difference Poisson's equation, and V_c is the volume of one grid cell.

Any fixed charge density can either be included in ρ and regarded as due to infinitely massive particles, or regarded as a contributor to $\phi_{\mathbf{j},\text{ext}}$.

The particle force is found from a potential energy V_i interpolated from ϕ:

$$\mathbf{F}_i = -\frac{\partial}{\partial \mathbf{x}_i} V_i(\mathbf{x}_i) = -q_i V_c \sum_{\mathbf{j}} \phi_{\mathbf{j}} \frac{\partial}{\partial \mathbf{x}_i} S(\mathbf{X}_{\mathbf{j}} - \mathbf{x}_i), \tag{3a}$$

$$V_i(\mathbf{x}_i) = q_i V_c \sum_{\mathbf{j}} \phi_{\mathbf{j}} S(\mathbf{X}_{\mathbf{j}} - \mathbf{x}_i). \tag{3b}$$

The gradient of S is performed analytically and is therefore exact. It is this step which differs crucially from the common algorithms, in which the potential is differentiated numerically and then interpolated. In addition to conserving energy, this change also brings about the predicted improved stability [2, 4].

In differentiating V_i, $\phi_{\mathbf{j}}$ is regarded as constant. In a code $\phi_{\mathbf{j}}$ is calculated from $\rho_{\mathbf{j}}$ in one step, and $\mathbf{F}_i$ is calculated in another step using that $\phi_{\mathbf{j}}$. It would not be convenient to compute an additional contribution involving $\partial\phi_{\mathbf{j}}/\partial\mathbf{x}_i$, nor is this necessary, as we shall see. The prescription given by Lewis, Eq. (50a) of [1], is identical to our (3a). We shall return to this point in Appendix A.

Note that the same interpolation function S is used in Eqs. 1 and 3b. Lewis gave examples using first-order (linear) interpolation in one dimension and in two (where it is also called bilinear or "area weighting" [5]). However, there was no restriction to this case in [1, 2]. Zero-order interpolation (nearest-grid-point), in which S is a discontinuous function, is not suitable because of the gradient in Eq. (3).

III. Energy Conservation

In this section we demonstrate the conservation of energy under rather general conditions on the field equations. Since the energy-conserving property applies exactly only when the time integration is exact for the particle equations of motion, we assume time is continuous in the following.

The rate of change of kinetic energy is

$$\begin{aligned}\frac{d}{dt} K.E. &= \frac{d}{dt} \sum_i \frac{1}{2} m_i \dot{\mathbf{x}}_i^2 = -\sum_i \dot{\mathbf{x}}_i \cdot \frac{\partial}{\partial \mathbf{x}_i} q_i V_c \sum_{\mathbf{j}} \phi_{\mathbf{j}} S(\mathbf{X}_{\mathbf{j}} - \mathbf{x}_i) \\ &= -V_c \sum_{\mathbf{j}} \phi_{\mathbf{j}} \frac{d}{dt} \sum_i q_i S(\mathbf{X}_{\mathbf{j}} - \mathbf{x}_i) \\ &= -V_c \sum \dot{\rho}_{\mathbf{j}} \phi_{\mathbf{j}}.\end{aligned} \tag{4}$$

By analogy with real electrostatic field theory, we expect that the potential energy of the system due to the fields of the particles will be [6]

$$\tfrac{1}{2}\sum_i V_{i,\text{self}}(\mathbf{x}_i),$$

where $V_{i,\text{self}}$ is interpolated from the first term of Eq. (2), and the potential energy due to the external potential will be $\sum V_{i,\text{ext}}$. Let us see when this is true. From the identity

$$\sum_i V_i(\mathbf{x}_i) \equiv V_c \sum_j \rho_j \phi_j , \tag{5}$$

which may be proven from Eqs. (1 and 3b), we find that the time rate of change of the prospective total energy is

$$\begin{aligned}\frac{d}{dt}\Big(K.E. + \frac{1}{2}\sum_i V_{i,\text{self}} + \sum_i V_{i,\text{ext}}\Big) &= \frac{d}{dt}\Big(K.E. + \frac{V_c}{2}\sum_j \rho_j\phi_{j,\text{self}} + V_c\sum_j \rho_j\phi_{j,\text{ext}}\Big) \\ &= V_c\sum_j \rho_j\dot{\phi}_{j,\text{ext}} + \frac{1}{2}V_c\sum_j(\rho_j\dot{\phi}_{j,\text{self}} - \dot{\rho}_j\phi_{j,\text{self}}).\end{aligned} \tag{6}$$

The first term on the right-hand side is the rate of change of total energy due to its explicit time dependence; it corresponds to $\partial H/\partial t$ and, therefore, its appearance is justified. To obtain an energy-conserving system, therefore, we want the second sum on the right-hand side to vanish.

That sum is zero if a discrete analogue to Green's reciprocation theorem exists, i.e., if

$$V_c \sum \rho_j^{(1)}\phi_{j,\text{self}}^{(2)} = V_c \sum \rho_j^{(2)}\phi_{j,\text{self}}^{(1)} \tag{7}$$

for any two density distributions $\rho^{(1)}$ and $\rho^{(2)}$ (just set $\rho^{(1)} = \rho$, $\rho^{(2)} = \dot{\rho}\, dt$). An alternate proof of the sufficiency of reciprocity for energy conservation is in Appendix A.

Such a theorem must exist with Lewis' prescription for the Poisson difference equation. Rewriting Eq. (60) in Ref. [1] in our notation,

$$4\pi\rho_j = V_c \sum_{j'} \phi_{j',\text{self}} \int d\mathbf{x}\left(\frac{\partial}{\partial \mathbf{x}} S(\mathbf{X}_{j'} - \mathbf{x})\right)\left(\frac{\partial}{\partial \mathbf{x}} S(\mathbf{X}_j - \mathbf{x})\right) \tag{8}$$

and substituting into Eq. (7) establishes the identity since the integral is invariant under interchange of subscripts j and j'. This latter property is very much less

restrictive than Eq. (8), and, therefore, the energy-conserving property is shared by a much wider class of algorithms than that derived by Lewis.

Equation (7) can be shown to be satisfied in other ways, e.g., if ϕ is given by Eq. (2) and the Green's function $g_{l,l}$ is known to be symmetric. In a neutral plasma with periodic boundary conditions and a Poisson equation which is symmetric to reflection in the lattice planes, the symmetry is ensured.[1] Another case is when the Poisson equation can be solved by a discrete Fourier transform, as in a periodic model, or with a square boundary at a fixed potential [1]; one requires only that the ratio $\phi(\mathbf{k})/\rho(\mathbf{k})$ be real [2]. If this ratio is positive, then the self-potential energy is nonnegative.

In more complicated model geometries one can at least check $g_{l,l}$ empirically. In any case it is clear that the energy-conserving property is easily obtained.

IV. Lewis' Poisson Difference Equation and the Coulomb Fields

While Lewis' prescription of the form of Poisson's equation is not related to energy conservation, it does attempt to reproduce accurately the Coulomb interaction implicit in his Lagrangian, even compensating partially for errors in interpolation. To see this we Fourier transform Eq. (8) using the conventions of [2, 4]:

$$K^2(\mathbf{k})\,\phi(\mathbf{k}) = 4\pi\rho(\mathbf{k}), \qquad K^2(\mathbf{k}) = \sum_{\mathbf{p}} k_{\mathbf{p}}^2 S^2(\mathbf{k}_{\mathbf{p}}^2). \tag{9ab}$$

In one dimension $k_p = k - 2\pi p/\Delta x$. (Note $K^2 \geqslant 0$, so the field energy is nonnegative.)

The particle density and force field are related by [2]

$$\mathbf{F}(\mathbf{k}) = -4\pi i q^2 \mathbf{k} S(\mathbf{k}) \sum_{\mathbf{p}} S(\mathbf{k}_{\mathbf{p}})\, n(\mathbf{k}_{\mathbf{p}}) \Big/ \sum_{\mathbf{p}} k_{\mathbf{p}}^2 S^2(\mathbf{k}_{\mathbf{p}}). \tag{10}$$

Suppose an interpolation is used which is free of "aliasing." This requires that $S(\mathbf{k}) = 0$ outside the first Brillouin zone, where the first zone is defined by $\max(k_x \Delta x, k_y \Delta y, k_z \Delta z) < \pi$ in a rectangular lattice. This is called "band-

[1] Formally, $g_{i,j} = g_{-i,-j} = g_{j,i}$. The first equality follows from reflection, the second from translation by the amount $i + j$. There is an arbitrariness in specifying g because the total charge is zero in a periodic system) so that a transformation of the g obtained straightforwardly from a Poisson solver may be required before the symmetries are explicit [7]. The relevance of symmetry is indicated by this example: Consider a single particle in an infinite system in which the Green's function is of the form $g_{i,j} \propto i - j$ (antisymmetric). Then the particle will accelerate in its own field gaining kinetic energy while the field energy is constant (zero).

limited" interpolation. It is not necessary that $S(\mathbf{k})$ be constant ($= 1$) within the first zone. In this case only the $\boldsymbol{p} = \mathbf{0}$ terms contribute, leaving

$$\begin{aligned} \mathbf{F}(\mathbf{k}) &= -4\pi i q^2 n(\mathbf{k})\, \mathbf{k}/k^2 \quad \text{in the first zone} \\ &= 0 \qquad \text{elsewhere.} \end{aligned}$$

Thus the long wavelengths are exact in the alias-free limit. If $S(\mathbf{k})$ is not constant in the first zone, so that there are errors in the interpolation, Lewis' Poisson algorithm makes compensating "errors" in calculating ϕ to yield good overall accuracy. This is important to the practical realization of high-accuracy algorithms, since if $S(\mathbf{k})$ is constant in the first zone then $S(\mathbf{x})$ drops off very slowly with increasing x and also does not remain positive.

Lindman has pointed out that small oscillations of a cold, nondrifting plasma in a linear-weighting Lewis model occur at exactly the correct frequency (except for time-integration errors). This interesting observation is true for any weighting function S, and in 1, 2, or 3 dimensions, as discussed in Appendix B. Here is an instance in which the variational principle does as well as can be done. However, this turns out to be an exceptional case, as will be seen.

As a measure of accuracy in realistic cases we examine the "averaged force" $\mathbf{F}_0(\mathbf{k})$, defined as follows [2]. Imagine holding the particles fixed while displacing (not rotating) the grid. Then $\mathbf{F}_0(\mathbf{x})$ is the average of $\mathbf{F}(\mathbf{x})$ over all such displacements. One can show that $\mathbf{F}_0(\mathbf{k})$ is obtained from Eq. (10) by keeping only the $\boldsymbol{p} = 0$ term in the numerator,

$$\mathbf{F}_0(\mathbf{k}) = -4\pi i q^2 n(\mathbf{k})\, \mathbf{k} \Big/ \sum_{\mathbf{p}} k_{\mathbf{p}}^2 S^2(\mathbf{k}_{\mathbf{p}}). \tag{11}$$

The applicability of $\mathbf{F}_0$ is discussed in [2] and in Appendix C. We will make use of it in Sects. VI and VII in discussing two examples.

V. Momentum Conservation

It has been mentioned elsewhere [2, 4, 8] that these models do not conserve momentum. We now show how this failure is associated with aliasing. Both are manifestations of the nonuniformity of the system dynamics. Consider the total force on the system of particles when band-limited interpolation is used:

$$\begin{aligned} \int d\mathbf{x}\, n(\mathbf{x})\, \mathbf{F}(\mathbf{x}) &= \int \frac{d\mathbf{k}}{(2\pi)^3}\, n(\mathbf{k})\, \mathbf{F}(-\mathbf{k}) \\ &= \int \frac{d\mathbf{k}}{(2\pi)^3}\, n(\mathbf{k})\, i\mathbf{k} S(\mathbf{k})\, q\phi(-\mathbf{k}) = \int \frac{d\mathbf{k}}{(2\pi)^3}\, i\mathbf{k}\rho(\mathbf{k})\, \phi(-\mathbf{k}) = 0, \end{aligned} \tag{12}$$

where $\rho(\mathbf{k}) = qS(\mathbf{k})n(\mathbf{k})$ in the absence of aliasing [2], and the integrand is odd. Thus the total particle force is zero and momentum is conserved. This is essentially because the particles can no longer sense the positions of the grid points; the nonuniformity of the grid is removed from the dynamics. (It should be noted that in the absence of aliasing the usual models, which conserve momentum, can be made to conserve energy also. See, e.g., Eq. (25) of [2] with K^2 defined as $k\kappa$ in the first zone.)

A simple instance of the failure of momentum conservation is the force exerted on a particle by its own field. We will examine this self-force later, but let us assume for the present that we are not interested in such a force error on the microscopic level (perhaps because it averages to zero) unless there is some macroscopic manifestation. We now give two examples in which a large change may take place in the total momentum.

An instability has been predicted [4] and observed [9] in a cold plasma drifting through the grid with a fixed neutralizing background. There need not be two or more plasma components drifting relative to each other. Clearly this instability is not physically valid; its origin is in aliasing errors. Let us divide the energy into three nonnegative parts: kinetic energy associated with the mean motion, kinetic energy of motion relative to the mean, and field energy. The sum of these can be

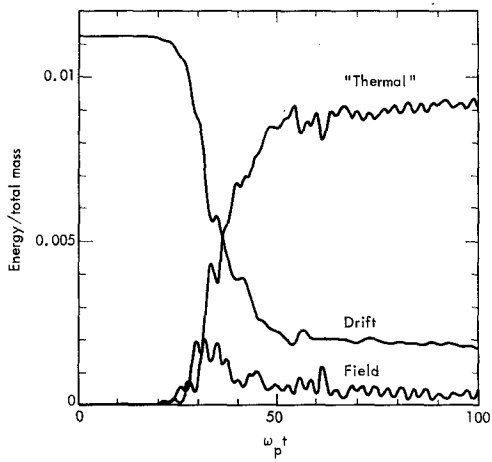

FIG. 1. This is an example of macroscopic failure of energy conservation. A cold beam passing through a fixed uniform neutralizing background is made unstable by the grid (via aliasing). Up to about $\omega_p t = 30$ the beam behaves as a linearized cold fluid. Drift kinetic energy ($\propto$ momentum^2) is converted to field energy and kinetic energy relative to the mean ("thermal" energy). Later behavior is more affected by the small number of particles used (960). The range of variation in the total energy is 0.6%; this variation is due to time integration errors ($\omega_p \Delta t = 0.1$). Other aspects of this computer run are shown in Fig. 2.

made to remain as nearly constant as desired, by decreasing the time step. As the instability develops, the latter two contributions to the total energy both increase, so the first contribution decreases. Therefore, the mean velocity and momentum must be decreasing. The force errors produce a drag on the mean motion. (Note that the existence of the energy constant means the instability amplitude is limited by the available energy, which is not the case for such instabilities in the usual models in which the total energy has been observed to increase several fold [9].) This description is supported by the simulation results shown in Figs. 1 and 2.

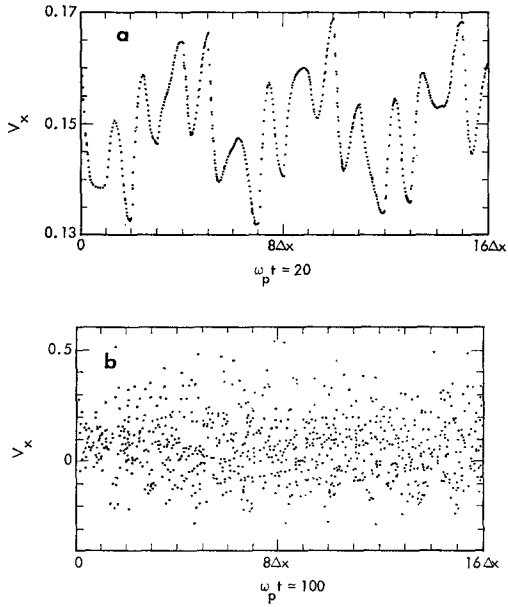

FIG. 2. This shows phase space at times $\omega_p t = 20$ and 100. The initial drift velocity was $0.15\ \omega_p \Delta x$ and the third mode was excited. Soon mode 13 [= number of grid points (16) minus fundamental mode number] appears. The two are coupled by the grid and grow quickly together (a). [Note the expanded velocity scale in (a)]. The distribution after saturation shows little structure (b).

Another example of a drag leading to decreasing momentum is predicted for a warm, uniform, stable plasma drifting through the grid [4, 8]. The loss of energy of mean motion is compensated for by an increase in temperature.

We do not claim to have shown that the lack of momentum conservation will necessarily be damaging in practice, but only that it can have macroscopically visible consequences.

VI. The Linear Interpolation Model Example

We now examine the nature of the particle force F in the linear interpolation examples [1]. First, we note that **F** is discontinuous. For given, fixed $\{\phi_j\}$ in two dimensions, F_x is continuous and piecewise linear as a function of y alone, and is a step function when x alone is varied. In one dimension, F is a step function[2]. Thus this case may be expected to be noisier than the algorithms known as CIC or PIC [10, 11] (but the overall computational time is shorter because the expression for **F** is much simpler). It may also be difficult to integrate in time accurately enough to realize an improvement in energy conservation. These questions have only begun to receive much empirical study [7].

Momentum Conservation and Self-Forces

As mentioned above, a simple example of the failure of momentum conservation is the force exerted on a particle by its own fields. This may be seen by considering a single particle in a large one-dimensional system, using linear interpolation. Place the particle between adjacent grid points located at $x = 0$ and Δx. Then the self-force is

$$\begin{aligned} F &= -q\,\frac{\phi_1 - \phi_0}{\Delta x} = 2\pi q \Delta x(\rho_0 - \rho_1) \\ &= -4\pi q^2\left(\frac{x}{\Delta x} - \frac{1}{2}\right), \qquad 0 \leqslant x \leqslant \Delta x. \end{aligned} \tag{13}$$

This is a simple harmonic oscillator potential well. Let us attempt to assess its importance in a single species plasma. It yields an oscillation frequency $\omega_{\text{self}} = \omega_p/\sqrt{n\Delta x}$ much smaller than the plasma frequency ω_p if the number of particles per cell $n\Delta x$ is large. The well depth energy, W_{self}, may be compared to the thermal energy [2]:

$$\frac{W_{\text{self}}}{(\frac{1}{2}mv_t^2)} = \frac{1}{4}\left(\frac{\Delta x}{\lambda_D}\right)^2 \Big/ (n\Delta x) = \frac{1}{4}\,(\Delta x/\lambda_D)/(n\lambda_D),$$

where m is the particle mass, v_t is the r.m.s. thermal velocity, and λ_D is the Debye length. These results have not been worked out exactly for two and three dimensions, but dimensional arguments indicate they would be

$$\frac{\omega_{\text{self}}^2}{\omega_p^2} \propto \frac{1}{N_c}, \text{ and } \frac{W_{\text{self}}}{\frac{1}{2}mv_t^2} \propto \frac{1}{N_c}\left(\frac{\Delta x}{\lambda_D}\right)^2, \tag{14ab}$$

[2] The force may be regarded as obtained by nearest-grid-point (NGP) "weighting" of an electric field $E_{j+1/2} = -(\phi_{j+1} - \phi_j)/\Delta x$.

where $N_c = nV_c$ is the number of particles per cell. The frequency ω_{self} is only an approximate indication of the average force gradient, since a single-particle oscillation is no longer simple harmonic.

Even if these ratios are small, one may wish in addition to have the self-force small compared to the macroscopic force of a wave field, say. This more stringent condition imposes a lower limit on wave amplitude, for a given density:

$$\text{(wave field energy)/(thermal energy)} \gtrsim N_c^{-2}(\Delta x/\lambda_D)^2 \tag{14c}$$

Note that all these ratios are desirably small when N_c is large, given $\Delta x/\lambda_D$. Furthermore, since the other particles in the cell each contribute forces comparable to a particle's self-force, the latter becomes relatively small compared to normal many-body interactions.

On the other hand, if Δx is decreased to zero holding n and λ_D constant then eventually W_{self} becomes so small that essentially all particles are untrapped. The oscillation superimposed on particle trajectories becomes small enough in amplitude and high enough in frequency that there is little interference with desired plasma behavior. In this limit the self-force is unimportant because its effect is averaged rapidly, although its average magnitude is unchanged.

We have so far ignored time-integration errors, in effect assuming the time step Δt is kept negligibly small. But if Δt is held constant while Δx is decreased then, when $\omega_{\text{self}}\,\Delta t \gtrsim 2$, the self-force oscillation becomes unstable. Particles will be thrown out of cells, never trapped. Even before the instability threshold, M. A. Lieberman has shown that particle velocities can diffuse without limit. This is of course an instance of gross nonconservation of energy, permitted by the time-integration errors.

While such unphysical behavior in even the "unperturbed" particle orbits is undesirable, one should compare it to velocity diffusion due to normal collisions. To estimate the self-force diffusion rate, assume Δx is so small that the particle's position in its cell is randomly and independently distributed from time step to step. The mean-square self-force in one dimension is $\langle F^2\rangle = 4\pi^2q^4/3$, leading to a diffusion given by

$$\langle \Delta v^2\rangle = \langle F^2\,\Delta t^2/m^2\rangle(t/\Delta t).$$

Defining a diffusion time τ_s by $\langle \Delta v^2\rangle = v_t^2$, we obtain

$$\omega_p\tau_s = 12\,\frac{(n\lambda_D)^2}{\omega_p\Delta t}, \tag{15}$$

whereas the normal collision times for a one dimensional plasma are $\omega_p\tau_c \sim (n\lambda_D)$ or $(n\lambda_D)^2$. There would seem to be no difficulty in making $\tau_s \gg \tau_c$, as desired. A similar argument may be made in two and three dimensions. Thus the time-

integration errors appear to increase the significance of the self-force, in this limit, but not disastrously.

One might try to restore momentum conservation by adding a new force to each particle which cancels its self-force. Apart from any other objections, this merely forces us to consider a more complicated example in order to observe the nonconservation of momentum. Consider two particles placed in the same cell. With the self-force cancelled the force on each is due solely to the fields of the other. Suppose for some placement of the two particles, the net force is zero. Displace particle 1, still keeping it in the same cell. This changes the potential field seen by particle 2. Then the force changes on particle 2 only. Thus the net force on the two is no longer zero and momentum is not conserved.

To see that no such approach will succeed, note that in the Vlasov limit the self-acceleration vanishes and the system is the same as without the self-force cancellation. The discussion of Sect. V shows that momentum is not conserved in the Vlasov limit.

A more subtle approach is to seek some smoothing (convolution) to apply to ρ_j and/or ϕ_j. Suppose ρ is convolved with A,

$$\rho_j' = \Delta x \sum_1 A_1 \rho_{j-1} , \tag{16}$$

and ρ' is used in Poisson's equation. Then one finds that the self-forces, and all interactions between particles in the same cell, have been decreased by the factor $\Delta x A_0$. (This should be taken as an indication of the effectiveness of smoothing, not as an invitation to set $A_0 = 0$. Then symptoms return when the two particles are in adjacent cells.)

The point is that the lack of conservation of momentum is not just a question

lower-order error in F_0 will reduce the order of overall accuracy. For linear weighting we find, using Eq. (8)

$$K^2/k^2 = S^2(k) + \frac{1}{12}(k\Delta x)^2 + O(\Delta x)^4.$$

Thus F_0 has a relative error $-(k\Delta x)^2/12$, causing a similar error in the oscillation frequency ω. Further, the error in Re ω can cause an error in Im ω by changing the phase velocity; for a Maxwellian, this contribution to relative error in Im ω is $-\Delta x^2/24\lambda_D^2$, independent of k.

This $O(\Delta x^2)$ error may be removed by changing the Poisson algorithm. One way to do this is to solve the same Poisson equation but with

$$\rho_j' = -\frac{1}{12}\rho_{j-1} + \frac{7}{6}\rho_j - \frac{1}{12}\rho_{j+1}$$

as the source density. One is then left with an $O(\Delta x^4)$ error in F_0 and from aliasing terms, resulting in a fourth order error in $\omega(k)$.

These remarks hold also in 2 or 3 dimensions. The Poisson algorithms proposed by Lewis [1] are not optimal from the present point of view. Whether they are optimal in some other situation (apart from the singular case of cold plasma oscillations) remains to be shown.

There should be no surprise that problems arise with the variational principle when the basis functions are an incomplete set. Many other such examples are known, e.g., Gibb's phenomenon in least-squares fitting of trigonometric sums (yielding a truncated Fourier series), in which, as here, better algorithms can be obtained after taking into account the nature of the result one is trying to compute.

VII. More Accurate Algorithms Using Splines

An "obvious" way to improve accuracy is to use higher-order Lagrange interpolation. But the second-order $S(\mathbf{x})$ is discontinuous and therefore unsuitable. Third order can be differentiated but yields a discontinuous force. Because of these discontinuities, $S(\mathbf{k})$ drops off slowly for large $\mathbf{k}$, implying poor aliasing properties.

If we arrange to have several continuous derivatives, then S will drop off more rapidly. This suggests the use of splines, which we now examine in the present formalism. Connection to the conventional spline-fitting problem is made in Appendix D.

Define $S_m(\mathbf{x})$ as the convolution of the square nearest-grid-point (NGP) weight-

ing function [2] with itself m times.[3] S_1 is the linear interpolation case above. The basis functions $S_m(\mathbf{X}_j - \mathbf{x})$, and therefore $V(\mathbf{x})$, are piecewise polynomials of order m. Derivatives exist through to order m, which is discontinuous. Note also that $S_m(\mathbf{x}) \geqslant 0$, which is not true for higher-order Lagrange interpolation.

The transform is

$$S_m(k) = \left(\frac{\sin \frac{1}{2}k\Delta x}{\frac{1}{2}k\Delta x}\right)^{m+1} \tag{17}$$

in one dimension. For large k, $S_m = O(k^{-m-1})$. At nonzero multiples of $k_g = 2\pi/\Delta x$, $S_m(k)$ has a zero of order $m + 1$, and so is expected to be small nearby. This is also true for Lagrange interpolation. However, for small k, $S(k \pm k_g)$ is about 5 times larger, and $S(k \pm 2k_g)$ about 21 times larger, for second order Lagrange than for S_2. Thus the spline reduces aliasing errors for long wavelengths yet takes the same amount of work to evaluate numerically. For small k, $S_m(k) \approx 1 - (m + 1)(k\Delta x)^2/24$, whereas $S - 1 = O(k^{m+1})$ or $O(k^{m+2})$ for Lagrange interpolation. However this "error" in the spline can be compensated for by the Poisson algorithm, as noted earlier.

Let us consider a complete algorithm for a one-dimensional periodic system. Cubic splines seem most common in other applications, but S_2 is computationally cheaper and is still a significant improvement over S_1. We have (see Fig. 3)

$$S_2(X_j - x) = \frac{1}{\Delta x}\left(\frac{3}{4} - \left(\frac{x - X_j}{\Delta x}\right)^2\right),$$

and (18)

$$S_2(X_{j\pm1} - x) = \frac{1}{2\Delta x}\left(\frac{1}{2} \pm \frac{x - X_j}{\Delta x}\right)^2, \text{ with } | x - X_j | \leqslant \Delta x/2.$$

The force may be regarded as obtained by linear interpolation of an electric field $E_{j+1/2} = -(\phi_{j+1} - \phi_j)/\Delta x$.

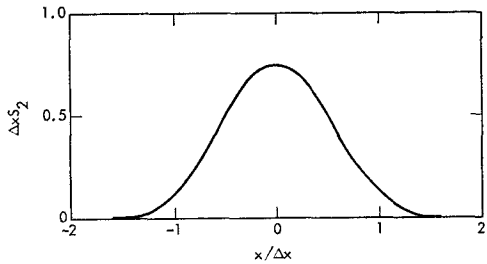

FIG. 3. The parabolic spline weighting function S_2 consists of 3 parabolic sections of length Δx, joined with no discontinuities in the derivative.

[3] For large m, S_m approaches a Gaussian in the sense of the central limit theorem. S_m is an analogue of the Gaussian for these systems.

The Poisson algorithm may be found from Eq. (8) following Lewis, or from Eqs. (9b, 17):

$$K^2(k) = \left(\frac{2}{\Delta x}\sin\frac{1}{2}k\Delta x\right)^6 \sum_p (k - pk_g)^{-4}$$
$$= \left(\frac{2}{\Delta x}\sin\frac{1}{2}k\Delta x\right)^2 \frac{1}{3}(2 + \cos k\Delta x), \tag{19}$$

where we have used the second derivative of Eq. 4.3.92 in [12]. This is all that is needed, if Fourier transform methods are to be used in the simulation.

For small k the relative "error" in both K^2 and S_2^2 is $-(k\Delta x)^2/4 + O(k^4)$, so that the second-order errors in $F_0(k)$ cancel (leaving a fourth-order relative error), showing how the long-wavelength errors due to S_1 have been reduced.

The difference-equation coefficients are the coefficients for an expansion of Eq. (19) in powers of $\exp(ik\Delta x)$:

$$-4\pi\rho_j \Delta x^2 = \tfrac{1}{6}(\phi_{j+2} + \phi_{j-2}) + \tfrac{1}{3}(\phi_{j+1} + \phi_{j-1}) - \phi_j . \tag{20}$$

This is a fourth-order difference equation, so that in a nonperiodic finite system two more boundary conditions are needed in addition to the usual two. These will emerge naturally from Eq. (60) in [1] and will depend on how the interpolation is modified at the ends of the system.

Equation (20) leads to a matrix equation in which the nonzero elements are all in a band five elements across down the diagonal, plus a few in the other corners. This can be solved quickly, but it may be advantageous to note that Eq. (19) shows how to solve two tridiagonal systems instead. Factoring K^2 leads to

$$\left(\frac{2}{\Delta x}\sin\frac{1}{2}k\Delta x\right)^2 \phi = -4\pi\rho', \qquad \frac{1}{3}(2 + \cos k\Delta x)\,\rho' = \rho. \tag{21ab}$$

The corresponding difference equations are

$$\tfrac{1}{6}\rho'_{j-1} + \tfrac{2}{3}\rho_j' + \tfrac{1}{6}\rho'_{j+1} = \rho_j , \tag{22a}$$

$$\phi_{j-1} - 2\phi_j + \phi_{j+1} = -4\pi\rho_j'\Delta x^2. \tag{22b}$$

The self-force in this example scales as in Eq. (14) but with a smaller constant multiple. In general the deficiencies due to aliasing (the instability, momentum nonconservation, grid noise) are expected to be reduced.

Returning to the question of oscillations of a warm plasma, we find that aliasing terms make a contribution to $\epsilon - \epsilon_0$ which is $O(\Delta x^6)$, while the error in F_0 is only fourth order. Again one achieves best accuracy in the complex frequency $\omega(k)$ with a Poisson algorithm different than that specified by the variational principle. One can show this to be true for splines of any order.

VIII. Conclusions

We have shown that the principal feature distinguishing the "energy-conserving" plasma simulation models is the derivation of the particle force from the grid potential. This is the same feature which eliminates some nonphysical instabilities present in the more common algorithms. Under very unrestrictive conditions on the Poisson difference operator, energy will be conserved and the field energy will be nonnegative. Thus, for example, the common practice of smoothing grid fields to suppress short wavelengths (and sometimes others as well) may be continued with these models.

Lewis' formalism does not take into account aliasing errors, so to understand it we consider the idealization in which the interpolation is free of aliasing (band-limited interpolation). It appears that only in this case is momentum conserved, and we find that the Coulomb field Fourier modes are exact for all wavelengths which can be represented unambiguously on the grid ($\mathbf{k}$ in the first Brillouin zone); Lewis' Poisson operator compensates for any remaining interpolation errors. In the practical examples of linear and parabolic weighting, aliasing errors spoil this compensating effect, and by one measure the Poisson difference equations given in [1] are unnecessarily inaccurate.

Total momentum changes considerably under some circumstances. In practice one may wish to monitor total momentum, just as total energy is often monitored in the usual models. The simplest manifestation of the failure of momentum conservation is the self-force. This force may not necessarily be troublesome. It may be reduced by smoothing the grid fields, which as said earlier will often be done for other reasons already.

To improve the accuracy of the algorithm, higher-order spline interpolation is clearly preferable to higher-order Lagrange interpolation. The parabolic spline model is derived in detail; it achieves improvement over the linear case, at some increase in computational expense.

Questions remain as to the advantages of these models, e.g., when time integration errors are taken into account, spoiling the exactness of energy conservation, but perhaps having less effect on the suppression of nonphysical instabilities. Empirical study is indicated.

APPENDIX A: Another Viewpoint on Energy Conservation

Lewis has suggested examining the force obtained as a gradient of the total potential energy. Using this would certainly lead to an energy-conserving code, but would be too expensive to compute. We wish to compare this force to that used in practice, given by Eq. (3a).

The gradient is

$$-\frac{\partial}{\partial \mathbf{x}_i}\text{P.E.} = -\frac{\partial}{\partial \mathbf{x}_i} V_c \sum_{\mathbf{j}} \left(\frac{1}{2}\rho_{\mathbf{j}}\phi_{\mathbf{j},\text{self}} + \rho_{\mathbf{j}}\phi_{\mathbf{j},\text{ext}}\right)$$

$$= -V_c \sum_{\mathbf{j}} \frac{\partial \rho_{\mathbf{j}}}{\partial \mathbf{x}_i}\phi_{\mathbf{j}} + \frac{V_c}{2}\sum_{\mathbf{j}}\left(\frac{\partial \rho_{\mathbf{j}}}{\partial \mathbf{x}_i}\phi_{\mathbf{j},\text{self}} - \rho_{\mathbf{j}}\frac{\partial \phi_{\mathbf{j},\text{self}}}{\partial \mathbf{x}_i}\right). \quad \text{(A.1)}$$

Using Eq. (1) the first term is seen to be the force of Eq. (3a). The second term is similar to the last term in Eq. (6), and vanishes when it does. There are two conclusions:

When there is reciprocity, as per Eq. (7), the force used in a code is identical to the negative gradient of the total field energy. This is a simple alternate proof that reciprocity leads to energy conservation. The discussion leading to Eq. (7) shows also that reciprocity is required.

(We can also show using reciprocity that if we had differentiated ϕ_j in Eq. (3a) we would have doubled the particle self forces.)

APPENDIX B: Small Oscillations of a Cold Plasma

In this appendix we show that small-amplitude oscillations of a cold plasma with no drift have the correct frequency and spatial properties. This is done with and without use of Fourier transforms.

The linear response of a cold fluid plasma is

$$n(\mathbf{k}, \omega) = in_0\mathbf{k}\cdot\mathbf{F}(\mathbf{k}, \omega)/m\omega^2. \quad \text{(B.1)}$$

We multiply this by $S(\mathbf{k})$, replace $\mathbf{F}$ using Eq. (10), replace $\mathbf{k}$ by $\mathbf{k}_{\mathbf{p}'}$, sum over $\mathbf{p}'$ making use of the periodicity of the sums in (10), then cancel the sums $\sum Sn$ and $\sum k_{\mathbf{p}}^2 S^2$. We are left with simply

$$\omega^2 = \frac{4\pi n_0 q^2}{m} \equiv \omega_p^2 \quad \text{(B.2)}$$

independent of $\mathbf{k}$. This is the correct result, having no error due to finite Δx.

Although this derivation is very short [once Eq. (10) has been derived] it is instructive to repeat the derivation *ab initio* without using Fourier transforms. The meaning of linearization and the fluid-limit will be clarified, as will the nature of the oscillations. For brevity the discussion will be kept to one dimension; the generalization is trivial.

wavelengths can be dominated by second-order errors in F_0 if the variational principle is used, as discussed at the end of Sect. VI.

The dispersion relation is [2, 4, 8]

$$\epsilon \equiv 1 + \frac{\omega_p^2}{K^2} \sum_{\mathbf{p}} S^2(\mathbf{k_p}) \int \mathbf{k_p} \cdot \frac{\partial f_0}{\partial \mathbf{v}} \frac{d\mathbf{v}}{\omega - \mathbf{k_p} \cdot \mathbf{v}}, \tag{C.1}$$

in which the particles are treated as a linearized Vlasov plasma, and $\mathbf{x}$, $\mathbf{v}$, and t are continuous. The effects of finite grid spacing are treated exactly. For simplicity we will work in one dimension.

If one keeps only the $\mathbf{p} = \mathbf{0}$ term in the above, one has an approximate relation which we will write as $\epsilon_0 = 0$ and which would be obtained if one started with F_0 as the interaction force. We will examine the difference between ϵ and ϵ_0, due to the aliasing terms.

In the linear weighting case we have

$$S^2(k_p) = \left(\frac{2}{k_p \Delta x} \sin \frac{k_p \Delta x}{2}\right)^4 = \left(\frac{k\Delta x}{2\pi p}\right)^4 \left(1 + \frac{2k\Delta x}{p\pi}\right) + O(k\Delta x)^6, \tag{C.2}$$

when $p \neq 0$ and $k\Delta x \ll \pi$. From this alone one suspects that $\epsilon - \epsilon_0$ is fourth order in Δx. To be sure we must consider the response of the plasma to short wavelengths by evaluating the velocity integral. We will use a Maxwellian with root-mean-square velocity spread v_t superimposed on a dirft velocity v_0. Then

$$\epsilon = 1 - \frac{1}{2K^2 {\lambda_D}^2} \sum_p S^2(k_p)\, Z'\left(\frac{\omega - k_p v_0}{\sqrt{2}\,|\,k_p\,|\,v_t}\right). \tag{C.3}$$

Z' is the derivative of the Fried–Conte plasma dispersion function [13]. We can proceed further analytically in the interesting case $\lambda_D \gtrsim \Delta x$, $v_0 \lesssim v_t$. Then the small argument expansion of Z' is appropriate:

$$\frac{1}{2} Z'\left(\frac{\xi}{\sqrt{2}}\right) = -i\sqrt{\frac{\pi}{2}}\, \xi e^{-\xi^2/2} - 1 + \xi^2 - \frac{1}{3}\xi^4 + \frac{1}{15}\xi^6 \cdots \tag{C.4}$$

Substituting this into Eq. (C.3) and using small-k expansions like (C.2) we have, to lowest nonvanishing order in Δx,

$$\epsilon - \epsilon_0 \approx \frac{1}{(k\lambda_D)^2} \left\{ \frac{(k\Delta x)^4}{720} + i2.65 \times 10^{-4} \frac{(k\Delta x)^5}{v_t} \left(\frac{\omega}{k} + 4v_0\right) \right\}. \tag{C.5}$$

The corresponding error in $\omega(k)$ is nearly proportional, so the errors in Re ω and Im ω are fourth and fifth order in Δx, respectively, due to aliasing. However,

using the variational principle, the error in F_0 is $O(\Delta x)^2$. An overall error of $O(\Delta x)^4$ in $\omega(k)$ requires a different Poisson operator, as discussed in Sect. VI.

As an aside, the imaginary part of Eq. (C.5) shows the damping influence of the aliasing terms when $v_0 = 0$. On the other hand, with $v_0 \neq 0$ these terms can become destabilizing. However instability is unlikely unless $v_0 \gtrsim v_t$; if we estimate $\omega = \omega_p + kv_0$ then aliasing is destabilizing if

$$| k | \lambda_D > \frac{1}{5} \left| \frac{v_t}{v_0} \right| .$$

But if $k\lambda_D$ is not small Landau damping will eliminate the instability.

APPENDIX D:
Relation to the Conventional Spline Interpolation Problem

The usual spline interpolation problem is to find a $V(x)$, given $V_j = V(X_j)$, which is piecewise polynomial and has a specified number of derivatives. We will use the same variables as in Eq. (3). In the common cubic case [$V(x)$ has a third derivative, which is discontinuous] one would solve

$$V_j = q\Delta x \sum_{j'} \phi_{j'} S_3(X_{j'} - X_j),$$

together with appropriate boundary conditions, as a set of simultaneous equations for the coefficients $\{\phi_j\}$ (Note that $V_j \neq q\phi_j$ for $m > 1$). The matrix is tridiagonal, with elements in the usual 1:4:1 ratio. The spline fit is then given by Eq. 3, except perhaps near the boundary. It is customary to specify the spline fit by means of the $\{V_j\}$ plus the derivatives $\{V_j'\}$ or $\{V_j''\}$, although our $\{\phi_j\}$ give a more compact specification.

APPENDIX E: Energy Calculation with Finite Time Step

Field and kinetic energies must be calculated from fields and velocities known at different times, when the usual "leap-frog" time integration is used. If we simply add the field energy to the kinetic energy at a time $\Delta t/2$ later, then this estimate of the total energy may be expected to be in error by approximately half the change per time step in the kinetic energy. This $O(\Delta t)$ error will usually be much larger than the $O(\Delta t^2)$ relative error in the time evolution of the system; so that it is an overly pessimistic diagnostic. Therefore, a simulation code should use some sort of time-centered average to obtain an energy diagnostic which has

an $O(\Delta t^2)$ error. We will consider several possibilities, using as an example a simple harmonic oscillator.

The leap-frog time integration is given by

$$\frac{x_{n+1} - x_n}{\Delta t} = v_{n+1/2}$$

$$\frac{v_{n+1/2} - v_{n-1/2}}{\Delta t} = -\omega_0^2 x_n$$

whose exact solution is

$$v_{n+1/2} = V \cos \omega t_{n+1/2}$$

$$x_n = \frac{V}{\omega_0} \sin \omega t_n$$

where $t_n = n\Delta t$ and $\omega_0 \Delta t/2 = \sin(\omega \Delta t/2)$. In the limit $\Delta t \to 0$, $\omega_0^2 x^2 + v^2 = V^2$, a constant. Several estimates of this energy are:

$$\omega_0^2 x_n^2 + v_{n\pm1/2}^2 = V^2 \mp \frac{1}{2} V^2(\omega_0 \Delta t) \sin 2\omega t_{n\pm1/4}\,, \tag{E.1}$$

$$\omega_0^2 x_n^2 + \left(\frac{v_{n-1/2} + v_{n+1/2}}{2}\right)^2 = V^2 - \frac{1}{8} V^2(\omega_0 \Delta t)^2 (1 + \cos 2\omega t_n), \tag{E.2}$$

$$\omega_0^2 x_n^2 + v_{n-1/2} v_{n+1/2} = V^2 - \frac{1}{4} V^2(\omega_0 \Delta t)^2, \tag{E.3}$$

$$\omega_0^2 x_n^2 + \frac{1}{2}(v_{n-1/2}^2 + v_{n+1/2}^2) = V^2 - \frac{1}{4} V^2(\omega_0 \Delta t)^2 \cos 2\omega t_n\,. \tag{E.4}$$

The first was discussed above. The kinetic energy in the other three is obtained from an arithmetic mean, geometric mean, and root mean square, respectively, of the previous and following velocities. The third has the advantage of being constant. The fourth has the advantage that it oscillates about the correct value, and the energy of a collection of many oscillators with random phases would be given correctly.

If the center of oscillation is drifting with velocity V_0, Eqs. (E.2–E.4) apply with the first term V^2 replaced by

$$V_0^2 + 2V_0 V \cos \frac{\omega \Delta t}{2} \cos \omega t_n + V^2$$

Therefore, there is no change in the comparison of their errors.

Another set of possibilities involves defining the energy at the half-steps and averaging the field energy. Two choices for this average are

$$\frac{V_c}{2} \sum_j \frac{1}{2} (\rho_{j,n}\phi_{j,n} + \rho_{j,n+1}\phi_{j,n+1}), \tag{E.5}$$

$$\frac{V_c}{2} \sum_j \rho_{j,n}\phi_{j,n+1} = \frac{V_c}{2} \sum_j \rho_{j,n+1}\phi_{j,n} . \tag{E.6}$$

The latter average has been suggested by O. Buneman. The former is positive definite, the latter is not. For instance, if one has a standing wave, then the field energy given by Eq. (E.6) will be negative when the fields change sign. This may be a nuisance, e.g., in making semilogarithmic plots of energy vs time. Kinetic energy calculated as per (E.3) also can be negative. However it is relatively unlikely that enough particles would reverse direction in the same time step to make the total kinetic energy of a system negative.

ACKNOWLEDGMENTS

Helpful conversations with H. R. Lewis and M. A. Lieberman are acknowledged.

REFERENCES

1. H. R. LEWIS, *J. Comp. Phys.* **6** (1970), 136; also "Methods in Computational Physics' (B. Alder, S. Fernbach, and M. Rotenberg, Eds.), Vol. 9, p. 307, Academic Press, New York 1970.
2. A. B. LANGDON, *J. Comp. Phys.* **6** (1970), 247.
3. E. L. LINDMAN, *J. Comp. Phys.* **5** (1970), 13.
4. A. B. LANGDON, report UCRL-72635, Lawrence Radiation Laboratory, Livermore, to be published in the "Proceedings of the Fourth Annual Conference on Numerical Simulation of Plasmas," held at the Naval Research Laboratory, Washington, D. C., Nov. 2–3, 1970.
5. F. H. HARLOW, *in* "Methods in Computational Physics" (B. Alder, S. Fernbach, and M. Rotenberg, Eds.), Vol. 3, p. 319, Academic Press, New York, 1964.
6. J. D. JACKSON, "Classical Electrodynamics," p. 21, Wiley, New York, 1962.
7. H. R. LEWIS, A. SYKES AND J. A. WESSON, *J. Comp. Phys.* **10** (1972), 85.
8. A. B. LANGDON, *in* "Third Quarterly Progress Report of 1970 on Plasma Research," Electronics Research Laboratory, University of California, Berkeley, CA, 1970.
9. H. OKUDA, "Proceedings of the Fourth Annual Conference on Numerical Simulation of Plasmas," held at the Naval Research Laboratory, Washington, D. C., Nov. 2–3, 1970, to be published; also *J. Comp. Phys.* **10** (1972), 475.
10. C. K. BIRDSALL AND D. FUSS, *J. Comp. Phys.* **3** (1969), 494.
11. R. L. MORSE, "Methods in Computational Physics" (B. Alder, S. Fernbach, and M. Rotenberg, Eds.), Vol. 9, p. 213, Academic Press, New York, 1970.

12. "Handbook of Mathematical Functions," (M. Abramowitz and I. A. Stegun, Eds.), U. S. Govt. Printing Office, Washington, D. C., 1964.
13. B. D. FRIED AND S. D. CONTE, "The Plasma Dispersion Function," Academic Press, New York, 1961.